Finite Element Response Sensitivity Analysis of Steel-Concrete Composite Beams with Deformable Shear Connection

A. Zona[1]; M. Barbato[2]; and J. P. Conte, M.ASCE[3]

Abstract: The behavior of steel-concrete composite beams is strongly influenced by the type of shear connection between the steel beam and the concrete slab. For accurate analytical predictions, the structural model must account for the interlayer slip between these two components. In numerous engineering applications (e.g., in the fields of structural optimization, structural reliability analysis, and finite element model updating), accurate response sensitivity calculations are needed as much as the corresponding response simulation results. This paper focuses on a procedure for response sensitivity analysis of steel-concrete composite structures using displacement-based locking-free frame elements including deformable shear connection with fiber discretization of the cross section. Realistic cyclic uniaxial constitutive laws are adopted for the steel and concrete materials as well as for the shear connection. The finite element response sensitivity analysis is performed according to the direct differentiation method. The concrete and shear connection material models as well as the static condensation procedure at the element level are extended for response sensitivity computations. Two steel-concrete composite structures for which experimental test results are available in the literature are used as realistic testbeds for response and response sensitivity analysis. These benchmark structures consist of a nonsymmetric, two-span continuous beam subjected to monotonic loading and a frame subassemblage under cyclic loading. The new analytical derivations for response sensitivity calculations and their computer implementation are validated through forward finite difference analysis based on the two benchmark examples considered. Selected sensitivity analysis results are shown for validation purposes and for quantifying the effect and relative importance of the various material parameters in regards to the nonlinear monotonic and cyclic response of the testbed structures.

DOI: 10.1061/(ASCE)0733-9399(2005)131:11(1126)

CE Database subject headings: Finite element method; Composite beams; Steel; Concrete; Connections; Sensitivity analysis.

Introduction

The last decade has seen a growing interest in finite element modeling and analysis of steel-concrete composite structures, with applications to seismic resistant frames and bridges (Spacone and El-Tawil 2004). The behavior of composite beams, made of two components connected through shear connectors to form an interacting unit, is significantly influenced by the type of connection between the steel beam and the concrete slab. Flexible shear connectors allow the development of partial composite action (Oehlers and Bradford 2000) and, for accurate analytical response predictions, structural models of composite structures must account for the interlayer slip between the steel and concrete components. Thus a composite beam finite element able to capture the interface slip is an essential tool for model-based response simulation of steel-concrete composite structures. The three-dimensional model for composite beams with deformable shear connection under a general state of stress developed by Dall'Asta (2001) simplifies to the model introduced by Newmark et al. (1951) if only the in-plane bending behavior is considered. In Newmark's model, the geometrically linear Euler-Bernoulli beam theory (i.e., small displacements, rotations, and strains) is used to model the two parts of the composite beam; the effects of the deformable shear connection are accounted for by using an interface model with distributed bond, while the contact between the steel and concrete components is enforced (Fig. 1). The interface slip is small since it is given by the difference in longitudinal displacements of the steel and concrete fibers at the steel-concrete interface.

Compared to common monolithic beams, composite beams with deformable shear connection present additional difficulties. Even in very simple structural systems (e.g., simply supported beams), complex distributions of the interface slip and force can develop; furthermore, these distributions can be very sensitive to the shear connection properties. Different finite elements representing composite beams with deformable shear connection have been proposed in the literature (Dall'Asta and Zona 2004a; Spacone and El-Tawil 2004). Despite the difficulties encountered in the nonlinear range of structural behavior, locking-free displacement-based elements (such as the one used in this study)

[1]Postgraduate Researcher, Dept. of Structural Engineering, Univ. of California at San Diego, 9500 Gilman Dr., La Jolla, CA 92093-0085. E-mail: azona@ucsd.edu

[2]Graduate Student, Dept. of Structural Engineering, Univ. of California at San Diego, 9500 Gilman Dr., La Jolla, CA 92093-0085. E-mail: mbarbato@ucsd.edu

[3]Professor, Dept. of Structural Engineering, Univ. of California at San Diego, 9500 Gilman Dr., La Jolla, CA 92093-0085 (corresponding author). E-mail: jpconte@ucsd.edu

Note. Associate Editor: Raimondo Betti. Discussion open until April 1, 2006. Separate discussions must be submitted for individual papers. To extend the closing date by one month, a written request must be filed with the ASCE Managing Editor. The manuscript for this paper was submitted for review and possible publication on August 23, 2004; approved on February 11, 2005. This paper is part of the ***Journal of Engineering Mechanics***, Vol. 131, No. 11, November 1, 2005. ©ASCE, ISSN 0733-9399/2005/11-1126–1139/$25.00.

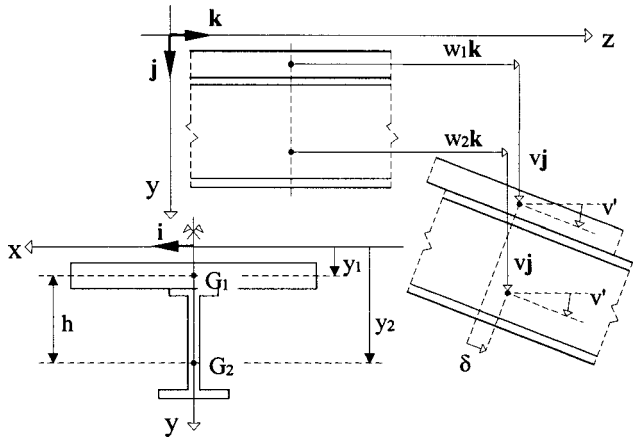

Fig. 1. Kinematics of two-dimensional composite beam model

produce accurate global and local results provided that the structure is properly discretized (Dall'Asta and Zona 2002, 2003, 2004a,b,c). Locking-free displacement-based elements were used successfully for accurate analysis of steel-concrete composite beam structures even in the case of very high gradients of the interface slip due, for example, to horizontal concentrated forces produced by external prestressing cables (Dall'Asta and Zona 2005).

Beyond research activities in model-based simulation of structures, recent years have seen a growing interest in the analysis of structural response sensitivity to various geometric, mechanical, and material properties defining the structure, and to loading parameters. Indeed, finite element response sensitivities represent an essential ingredient for gradient-based optimization methods needed in various subfields of structural engineering such as structural optimization, structural reliability analysis, structural identification, and finite element model updating (Ditlevsen and Madsen 1996; Kleiber et al. 1997). In addition, finite element response sensitivities are invaluable for gaining deeper insight into the effect and relative importance of system and loading parameters in regards to structural response behavior.

This paper focuses on materially nonlinear-only static response sensitivity analysis using displacement-based, locking-free finite elements for composite beams with deformable shear connection (Dall'Asta and Zona 2002). Realistic uniaxial cyclic constitutive laws are adopted for the steel and concrete materials of the beam and for the shear connection. The monotonic and cyclic responses of these materials and resulting finite element models are validated through comparison with experimental test results available in the literature (Ansourian 1981; Bursi and Gramola 2000). The finite element response sensitivity analysis is performed following the direct differentiation method (DDM) and validated by means of forward finite difference (FFD) analysis (Conte 2001; Conte et al. 2003) in the context of two realistic steel-concrete testbed structures considered in this study. The first benchmark structure consists of a nonsymmetric two-span continuous beam subjected to a monotonically increasing concentrated force, while the second benchmark structure is a frame subassemblage under cyclic loading. Results of sensitivity analysis are used to investigate and quantify the effect and relative importance of the various material parameters in regards to the monotonic and cyclic nonlinear response of the two testbed structures considered.

Response Sensitivity Analysis by the Direct Differentiation Method

Introduction

If r denotes a generic scalar response quantity (e.g., displacement, strain, stress), then by definition, the sensitivity of r with respect to the material or loading parameter θ is expressed mathematically as the absolute partial derivative of r with respect to the variable θ, $\partial r/\partial\theta|_{\theta=\theta_0}$, where θ_0 denotes the nominal value taken by the sensitivity parameter θ for the finite element response analysis.

In the sequel, following the notation proposed by Kleiber et al. (1997), the scalar response quantity $r(\boldsymbol{\vartheta})=r[\mathbf{f}(\boldsymbol{\vartheta}),\boldsymbol{\vartheta}]$ depends on the parameter vector $\boldsymbol{\vartheta}$ (defined by n time-independent sensitivity parameters, i.e., $\boldsymbol{\vartheta}=[\theta_1\cdots\theta_n]^T$) both explicitly and implicitly through the vector function $\mathbf{f}(\boldsymbol{\vartheta})$. According to the notation adopted herein, $dr/d\boldsymbol{\vartheta}$ denotes the gradient or total derivative of r with respect to $\boldsymbol{\vartheta}$, $dr/d\theta_i$ represents the absolute partial derivative of the response quantity r with respect to the scalar variable θ_i, $i=1,\ldots,n$ (i.e., the derivative of r with respect to parameter θ_i considering both explicit and implicit dependencies of r on θ_i), and $\partial r/\partial\theta_i|_{\mathbf{z}}$ denotes the partial derivative of r with respect to parameter θ_i when the vector of variables $\mathbf{z}$ is kept constant (fixed). In the particular and important case in which $\mathbf{z}=\mathbf{f}(\boldsymbol{\vartheta})$, the expression $\partial r/\partial\theta_i|_{\mathbf{z}}$ reduces to the partial derivative of r considering only the explicit dependency of r on parameter θ_i. For $\boldsymbol{\vartheta}=\theta=\theta_1$ (case of a single sensitivity parameter), the adopted notation reduces to the usual elementary calculus notation. The derivations below consider the case of a single (scalar) sensitivity parameter θ without loss of generality, due to the uncoupled nature of the sensitivity equations with respect to different sensitivity parameters.

Following the direct differentiation method (DDM) (Conte 2001; Conte et al. 2003), the consistent finite element response sensitivities are computed at each time step, after convergence is achieved for the response computation. This requires the exact differentiation of the finite element algorithm for the response calculation (including the numerical integration scheme for the material constitutive law) with respect to the sensitivity parameter θ. Consequently, the response sensitivity calculation algorithm affects the various hierarchical layers of finite element response calculation, namely: (1) the structure level, (2) the element level, (3) the section level, and (4) the material level.

Response Sensitivity Analysis at the Structure Level

After spatial discretization using the finite element method, the equilibrium equations of a materially nonlinear-only model of a structural system subjected to quasi-static loading condition can be expressed as

$$\mathbf{R}[\mathbf{u}(t,\theta),\theta]=\mathbf{F}(t,\theta) \tag{1}$$

where t=pseudotime; θ=scalar sensitivity parameter (material or loading variable); $\mathbf{u}$=vector of nodal displacements; $\mathbf{R}$=history dependent structure internal resisting force vector; and $\mathbf{F}$=applied quasi-static load vector. The solution $\mathbf{u}_{n+1}$ of Eq. (1) at discrete time t_{n+1} is obtained through the Newton–Raphson iterative procedure, which consists of solving a linearized system of equations at each iteration, until equilibrium between discrete external and internal resisting forces, i.e.

$$\mathbf{F}_{n+1} - \mathbf{R}(\mathbf{u}_{n+1}) = \mathbf{0} \tag{2}$$

is satisfied within a prescribed tolerance. In the above equations, the subscript "$n+1$" indicates that the quantity to which it is attached is evaluated at time t_{n+1}. The problem can be easily extended to the case of dynamic loading by adding inertial and damping forces in Eq. (1) and integrating the resulting equations of motion using a time-stepping scheme such as the Newmark-β method, which yields a linearized equation similar to Eq. (2) (Conte 2001; Conte et al. 2003, 2004).

Assuming that $\mathbf{u}_{n+1}$ is the converged solution (up to some iteration residuals satisfying a specified tolerance) at discrete time t_{n+1}, and differentiating Eq. (2) with respect to θ using the chain rule of differentiation (recognizing the explicit and implicit dependence of $\mathbf{R}$ on θ), the following response sensitivity equation at the structure level is obtained (Conte et al. 2003):

$$(\mathbf{K}_T^{\text{stat}})_{n+1} \frac{d\mathbf{u}_{n+1}}{d\theta} = \frac{d\mathbf{F}_{n+1}}{d\theta} - \left. \frac{\partial \mathbf{R}[\mathbf{u}_{n+1}(\theta), \theta]}{\partial \theta} \right|_{\mathbf{u}_{n+1}} \tag{3}$$

where $\mathbf{K}_T^{\text{stat}}$ = structure consistent (or algorithmic) tangent stiffness matrix at the converged state at time t_{n+1}. The second term on the right-hand side (RHS) of Eq. (3) represents the partial derivative of the structure internal resisting force vector, $\mathbf{R}(\mathbf{u}_{n+1})$, with respect to sensitivity parameter θ under the condition that the displacement vector $\mathbf{u}_{n+1}$ remains fixed (conditional derivative). It can be expressed as

$$\left. \frac{\partial \mathbf{R}[\mathbf{u}_{n+1}(\theta), \theta]}{\partial \theta} \right|_{\mathbf{u}_{n+1}} = \mathop{\mathbf{A}}_{e=1}^{\text{Nel}} \left\{ \left. \frac{\partial \mathbf{Q}_{n+1}^{(e)}[\mathbf{q}_{n+1}^{(e)}(\theta), \theta]}{\partial \theta} \right|_{\mathbf{q}_{n+1}^{(e)}} \right\} \tag{4}$$

where $\mathbf{A}_{e=1}^{\text{Nel}}\{\cdots\}$ denotes the direct stiffness assembly operator from the element level (in local element coordinates) to the structure level in global coordinates; Nel represents the total number of finite elements in the structural model; $\mathbf{Q}_{n+1}^{(e)}$ = element internal resisting force vector; and $\mathbf{q}_{n+1}^{(e)}$ = vector of element nodal displacements in local coordinates.

Once the RHS of Eq. (3) has been formed, the vector of nodal displacement sensitivities, $d\mathbf{u}_{n+1}/d\theta$, can be solved; subsequently, the unconditional derivatives of all history/state variables at the element, section, and material levels at all integration points are updated as described in the following sections.

Notice that, once the numerical response of the structural system is known at time t_{n+1}, the matrix sensitivity equation, Eq. (3), is linear and has the same left-hand-side (LHS) matrix operator (consistent tangent stiffness matrix) as the consistently linearized global equilibrium equations at the end of the iteration which satisfies convergence for the response calculation at time t_{n+1}. Therefore only the RHS of Eq. (3) needs to be recomputed and since the factorization of the consistent tangent stiffness matrix is already available at the converged time step t_{n+1}, computation of the response sensitivities by solving Eq. (3) is very efficient. The RHS of Eq. (3) is recomputed and Eq. (3) is solved for as many sensitivity parameters θ_i as needed.

Response Sensitivity Analysis at the Element Level

The calculation of the conditional derivative of the element resisting force vector on the RHS of Eq. (4) is performed at the element level. Since displacement-based locking-free frame elements for composite beams with deformable shear connection have internal nodes (Dall' Asta and Zona 2004b), the element internal resisting force vector needed to assemble the structure resisting force vector is obtained after static condensation of the internal degrees of freedom (DOFs). The static condensation of the internal DOFs is an algebraic procedure (Bathe 1995), corresponding to a partial Gauss elimination, commonly used in finite elements with internal nodes (or DOFs) in order to reduce the size of the system of equilibrium equations to be solved at the structure level.

The element nodal displacement vector $\mathbf{q}$ and element nodal resisting force vector $\mathbf{Q}$ can be partitioned according to the external (subscript e) and internal (subscript i) DOFs as

$$\mathbf{q} = \begin{bmatrix} \mathbf{q}_e \\ \mathbf{q}_i \end{bmatrix} \quad \text{and} \quad \mathbf{Q} = \begin{bmatrix} \mathbf{Q}_e \\ \mathbf{Q}_i \end{bmatrix} \tag{5}$$

The linearized incremental equilibrium equations at the element level can be written in partitioned form as

$$\begin{bmatrix} \mathbf{K}_{ee} & \mathbf{K}_{ei} \\ \mathbf{K}_{ie} & \mathbf{K}_{ii} \end{bmatrix} \begin{bmatrix} \delta\mathbf{q}_e \\ \delta\mathbf{q}_i \end{bmatrix} = \begin{bmatrix} \mathbf{F}_e - \mathbf{Q}_e \\ \mathbf{F}_i - \mathbf{Q}_i \end{bmatrix} \tag{6}$$

where $\delta\mathbf{q}_e$ and $\delta\mathbf{q}_i$ represent linearized increments of $\mathbf{q}_e$ and $\mathbf{q}_i$, respectively; $\mathbf{F}_e$ and $\mathbf{F}_i$ denote the quasi-static load vectors corresponding to the external and internal DOFs, respectively; and the submatrices of the element tangent stiffness matrix are defined as

$$\mathbf{K}_{ee} = \left. \frac{\partial \mathbf{Q}_e}{\partial \mathbf{q}_e} \right|_\theta, \quad \mathbf{K}_{ei} = \left. \frac{\partial \mathbf{Q}_e}{\partial \mathbf{q}_i} \right|_\theta,$$

$$\mathbf{K}_{ie} = \left. \frac{\partial \mathbf{Q}_i}{\partial \mathbf{q}_e} \right|_\theta = \mathbf{K}_{ei}^T, \quad \mathbf{K}_{ii} = \left. \frac{\partial \mathbf{Q}_i}{\partial \mathbf{q}_i} \right|_\theta \tag{7}$$

where the conditioning on θ expresses the fact that these vector function derivatives are evaluated for the unperturbed sensitivity parameter θ. In Eq. (6), it should be noted that $\mathbf{F}_e$ also includes the effects of external distributed loads and internal resisting forces acting over and within adjacent finite elements. After condensation of the internal DOFs, Eq. (6) reduces to

$$\mathbf{K}_c \delta\mathbf{q}_c = \mathbf{F}_c - \mathbf{Q}_c \tag{8}$$

where $\mathbf{q}_c = \mathbf{q}_e$ ($\rightarrow \delta\mathbf{q}_c = \delta\mathbf{q}_e$), and

$$\mathbf{K}_c = \mathbf{K}_{ee} - \mathbf{K}_{ei}\mathbf{K}_{ii}^{-1}\mathbf{K}_{ie}$$

$$\mathbf{F}_c = \mathbf{F}_e - \mathbf{K}_{ei}\mathbf{K}_{ii}^{-1}\mathbf{F}_i$$

$$\mathbf{Q}_c = \mathbf{Q}_e - \mathbf{K}_{ei}\mathbf{K}_{ii}^{-1}\mathbf{Q}_i \tag{9}$$

In the above equations, $\mathbf{K}_c$ = condensed element tangent stiffness matrix; $\mathbf{F}_c$ = condensed quasi-static load vector; and $\mathbf{Q}_c$ = condensed internal resisting force vector. At convergence of the response calculation at time t_{n+1}, the incremental quantities $\delta\mathbf{q}_e$, $\delta\mathbf{q}_i$, and $\delta\mathbf{q}_c$ in Eqs. (6) and (8) reduce to zero (within a small finite precision dependent on the prescribed tolerance) and the quantities appearing in Eq. (9) must be considered as computed at time t_{n+1}. In particular, this implies that the matrices $\mathbf{K}_{ee}$, $\mathbf{K}_{ei}$, $\mathbf{K}_{ie}$, $\mathbf{K}_{ii}$, and $\mathbf{K}_c$ are consistent tangent stiffness matrices obtained through consistent linearization of the equilibrium equations at time t_{n+1}. Thus they must be considered as constant quantities with respect to $\mathbf{q}_e$, $\mathbf{q}_i$, $\mathbf{q}_c$ (since they are linearizing constants) and θ (since evaluated at $\theta = \theta_0$).

After static condensation, Eq. (4) reduces to

$$\left.\frac{\partial \mathbf{R}_c[\mathbf{u}_{n+1}(\theta),\theta]}{\partial\theta}\right|_{\mathbf{u}_{n+1}} = \mathop{\mathbf{A}}_{e=1}^{\text{Nel}}\left\{\left.\frac{\partial \mathbf{Q}^{(e)}_{c,n+1}[\mathbf{q}^{(e)}_{n+1}(\theta),\theta]}{\partial\theta}\right|_{\mathbf{q}^{(e)}_{n+1}}\right\} \tag{10}$$

where $\mathbf{R}_c$ denotes the condensed vector of structure resisting forces. In the following, the subscript "$n+1$" is omitted for the sake of brevity.

Differentiating Eq. (9) (third line) with respect to $\mathbf{q}_i$ for θ fixed and using Eq. (7) yields

$$\left.\frac{\partial \mathbf{Q}_c}{\partial \mathbf{q}_i}\right|_\theta = \left.\frac{\partial \mathbf{Q}_e}{\partial \mathbf{q}_i}\right|_\theta - \mathbf{K}_{ei}\mathbf{K}_{ii}^{-1}\left.\frac{\partial \mathbf{Q}_i}{\partial \mathbf{q}_i}\right|_\theta = \mathbf{K}_{ei} - \mathbf{K}_{ei}\mathbf{K}_{ii}^{-1}\mathbf{K}_{ii} = \mathbf{0} \tag{11}$$

The above equation indicates that $\mathbf{Q}_c$ is independent of $\mathbf{q}_i$ for θ fixed. Thus

$$\mathbf{Q}_c = \mathbf{Q}_c[\mathbf{q}_e(\theta),\theta] \tag{12}$$

Differentiating Eq. (9) (third line) with respect to θ gives

$$\frac{d\mathbf{Q}_c}{d\theta} = \frac{d\mathbf{Q}_e}{d\theta} - \mathbf{K}_{ei}\mathbf{K}_{ii}^{-1}\frac{d\mathbf{Q}_i}{d\theta} \tag{13}$$

Differentiating Eq. (12) with respect to θ using the implicit function theorem of differentiation results in

$$\frac{d\mathbf{Q}_c}{d\theta} = \left.\frac{\partial \mathbf{Q}_c}{\partial \mathbf{q}_e}\right|_\theta \frac{d\mathbf{q}_e}{d\theta} + \left.\frac{\partial \mathbf{Q}_c}{\partial\theta}\right|_{\mathbf{q}} \tag{14}$$

which can be rewritten as, using Eqs. (9) (first line) and (9) (third line)

$$\frac{d\mathbf{Q}_c}{d\theta} = \mathbf{K}_c\frac{d\mathbf{q}_e}{d\theta} + \left.\frac{\partial \mathbf{Q}_c}{\partial\theta}\right|_{\mathbf{q}} \tag{15}$$

In Eq. (15), the only term that remains to be derived is $\partial\mathbf{Q}_c/\partial\theta|_{\mathbf{q}}$. This term is extremely important, since it is needed to assemble the conditional derivative/sensitivity of the condensed internal resisting force vector at the structure level as expressed in Eq. (10). It is computed through substituting Eq. (13) into Eq. (15) after solving for $d\mathbf{Q}_e/d\theta$ and $d\mathbf{Q}_i/d\theta$ as follows.

In general, we have the following functional dependence of vectors $\mathbf{Q}_e$ and $\mathbf{Q}_i$ on the sensitivity parameter θ:

$$\mathbf{Q}_e = \mathbf{Q}_e[\mathbf{q}_e(\theta),\mathbf{q}_i(\theta),\theta]$$

$$\mathbf{Q}_i = \mathbf{Q}_i[\mathbf{q}_e(\theta),\mathbf{q}_i(\theta),\theta] \tag{16}$$

Applying the implicit function theorem of differentiation to Eq. (16) yields

$$\begin{aligned}\frac{d\mathbf{Q}_e}{d\theta} &= \left.\frac{\partial \mathbf{Q}_e}{\partial \mathbf{q}_e}\right|_\theta \frac{d\mathbf{q}_e}{d\theta} + \left.\frac{\partial \mathbf{Q}_e}{\partial \mathbf{q}_i}\right|_\theta \frac{d\mathbf{q}_i}{d\theta} + \left.\frac{\partial \mathbf{Q}_e}{\partial\theta}\right|_{\mathbf{q}} \\ &= \mathbf{K}_{ee}\frac{d\mathbf{q}_e}{d\theta} + \mathbf{K}_{ei}\frac{d\mathbf{q}_i}{d\theta} + \left.\frac{\partial \mathbf{Q}_e}{\partial\theta}\right|_{\mathbf{q}} \\ \frac{d\mathbf{Q}_i}{d\theta} &= \left.\frac{\partial \mathbf{Q}_i}{\partial \mathbf{q}_e}\right|_\theta \frac{d\mathbf{q}_e}{d\theta} + \left.\frac{\partial \mathbf{Q}_i}{\partial \mathbf{q}_i}\right|_\theta \frac{d\mathbf{q}_i}{d\theta} + \left.\frac{\partial \mathbf{Q}_i}{\partial\theta}\right|_{\mathbf{q}} \\ &= \mathbf{K}_{ie}\frac{d\mathbf{q}_e}{d\theta} + \mathbf{K}_{ii}\frac{d\mathbf{q}_i}{d\theta} + \left.\frac{\partial \mathbf{Q}_i}{\partial\theta}\right|_{\mathbf{q}}\end{aligned} \tag{17}$$

After solving the matrix sensitivity equation at the structure level, Eq. (3), only the unconditional derivatives, $d\mathbf{q}_e/d\theta$, of the element external DOFs in local coordinates are known. Thus it is necessary to compute at the element level the unconditioned derivatives, $d\mathbf{q}_i/d\theta$, of the element internal DOFs in local coordinates. In fact, the unconditioned sensitivities of the history/state variables at the section level can be updated only if the unconditional derivatives of all the element DOFs (external and internal) are known.

Eq. (2) written at the element level implies that the following relations are verified at convergence:

$$\mathbf{Q}_e - \mathbf{F}_e = \mathbf{0}$$

$$\mathbf{Q}_i - \mathbf{F}_i = \mathbf{0} \tag{18}$$

where the zero equalities are satisfied up to some iteration residuals. Differentiating Eq. (18) (second line) with respect to θ yields

$$\frac{d\mathbf{Q}_i}{d\theta} - \frac{d\mathbf{F}_i}{d\theta} = \mathbf{0} \tag{19}$$

The term $d\mathbf{F}_i/d\theta$ depends only on the distributed and/or concentrated external forces applied on the internal nodes. Therefore $d\mathbf{F}_i/d\theta$ and consequently $d\mathbf{Q}_i/d\theta$ can be considered as known and if the parameter θ is not related to the element distributed loads, we have

$$\frac{d\mathbf{F}_i}{d\theta} = \frac{d\mathbf{Q}_i}{d\theta} = \mathbf{0} \tag{20}$$

Substituting Eq. (20) into Eq. (17) (second line) and solving for $d\mathbf{q}_i/d\theta$ yields

$$\frac{d\mathbf{q}_i}{d\theta} = \mathbf{K}_{ii}^{-1}\left(\frac{d\mathbf{Q}_i}{d\theta} - \mathbf{K}_{ie}\frac{d\mathbf{q}_e}{d\theta} - \left.\frac{\partial \mathbf{Q}_i}{\partial\theta}\right|_{\mathbf{q}}\right) \tag{21}$$

Substituting Eq. (21) into Eq. (17) (first line) and performing some algebraic manipulations yield

$$\begin{aligned}\frac{d\mathbf{Q}_e}{d\theta} - \mathbf{K}_{ei}\mathbf{K}_{ii}^{-1}\frac{d\mathbf{Q}_i}{d\theta} &= (\mathbf{K}_{ee} - \mathbf{K}_{ei}\mathbf{K}_{ii}^{-1}\mathbf{K}_{ie})\frac{d\mathbf{q}_e}{d\theta} \\ &+ \left(\left.\frac{\partial \mathbf{Q}_e}{\partial\theta}\right|_{\mathbf{q}} - \mathbf{K}_{ei}\mathbf{K}_{ii}^{-1}\left.\frac{\partial \mathbf{Q}_i}{\partial\theta}\right|_{\mathbf{q}}\right)\end{aligned} \tag{22}$$

By comparing Eq. (22) with Eq. (15), using Eq. (13), we deduce that

$$\left.\frac{\partial \mathbf{Q}_c}{\partial\theta}\right|_{\mathbf{q}} = \left.\frac{\partial \mathbf{Q}_e}{\partial\theta}\right|_{\mathbf{q}} - \mathbf{K}_{ei}\mathbf{K}_{ii}^{-1}\left.\frac{\partial \mathbf{Q}_i}{\partial\theta}\right|_{\mathbf{q}} \tag{23}$$

The conditional derivatives $\partial\mathbf{Q}_e/\partial\theta|_\theta$ and $\partial\mathbf{Q}_i/\partial\theta|_\theta$ are obtained as

$$\begin{bmatrix}\left.\frac{\partial \mathbf{Q}_e}{\partial\theta}\right|_{\mathbf{q}} \\ \left.\frac{\partial \mathbf{Q}_i}{\partial\theta}\right|_{\mathbf{q}}\end{bmatrix} = \left.\frac{\partial \mathbf{Q}[\mathbf{q}(\theta),\theta]}{\partial\theta}\right|_{\mathbf{q}} = \int_0^L \mathbf{B}^T(z)\left.\frac{\partial \mathbf{D}[\mathbf{B}(z)\cdot\mathbf{q}(\theta),\theta]}{\partial\theta}\right|_{\mathbf{q}} dz \tag{24}$$

where $\mathbf{D}$ denotes the vector of active stress resultants at the section level and $\mathbf{B}$=transformation matrix between the vector of element nodal displacements $\mathbf{q}$ and the vector of generalized section deformations $\mathbf{d}$ [i.e., compatibility equation $\mathbf{d}(z,\theta)=\mathbf{B}(z)\cdot\mathbf{q}(\theta)$]. The calculation of the conditional derivative on the RHS of Eq. (24) is carried out at the section level.

Response Sensitivity Analysis at the Section Level

In the case of a composite beam with deformable shear connection, the vector of generalized section deformations is defined as (Dall'Asta and Zona 2004a)

$$\mathbf{d}^T(z,\theta) = [\varepsilon_1(z,\theta)\ \varepsilon_2(z,\theta)\ \chi(z,\theta)\ \delta(z,\theta)] \tag{25}$$

where ε_1 and ε_2=axial strains at the reference points G_1 (concrete slab) and G_2 (steel beam), respectively (Fig. 1); χ=curvature (same for concrete slab and steel beam); and δ=slip at the interface between the concrete slab and the steel beam. The vector of section stress resultants is defined as (Dall'Asta and Zona 2004a)

$$\mathbf{D}^T(z,\theta) = [N_1(z,\theta)\ N_2(z,\theta)\ M_{12}(z,\theta)\ f_s(z,\theta)] \tag{26}$$

where N_1=axial force in the concrete slab; N_2=axial force in the steel beam; M_{12}=summation of the bending moments in the concrete slab and steel beam; and f_s=interface shear force per unit length. The stress resultants N_1, N_2, and M_{12} are calculated through numerical integration over the concrete and steel parts of the beam cross section, which are discretized using a fiber model.

The calculation of the conditional derivative (for **q** fixed and therefore for **d** fixed) of the vector of section stress resultants in Eq. (24) is carried out as

$$\left.\frac{\partial N_\alpha}{\partial\theta}\right|_{\mathbf{d}} = \int_{A_\alpha} \left.\frac{\partial\sigma[y,\varepsilon_\alpha(z,\theta),\chi(z,\theta),\theta]}{\partial\theta}\right|_{\mathbf{d}} dA, \quad \alpha = 1,2 \tag{27}$$

$$\left.\frac{\partial M_{12}}{\partial\theta}\right|_{\mathbf{d}} = \sum_{\alpha=1}^{2}\left\{\int_{A_\alpha}(y-y_\alpha)\left.\frac{\partial\sigma[y,\varepsilon_\alpha(z,\theta),\chi(z,\theta),\theta]}{\partial\theta}\right|_{\mathbf{d}} dA\right\} \tag{28}$$

where σ=normal stress; y_1 and y_2=reference points of the two components of the composite beam (Fig. 1); and A_1 and A_2=cross-section areas of the concrete slab and steel beam, respectively. The conditional derivative on the RHS of Eqs. (27) and (28) and the conditional derivative of f_s (given **d**) are calculated at the material level, hence the (discretized) material constitutive equations must be defined and differentiated analytically with respect to the sensitivity parameter θ.

After solving the sensitivity equations at the structure level, Eq. (3) in condensed form, for $d\mathbf{u}_{n+1}/d\theta$ and calculating the unconditional derivatives of the displacements at the (external and internal) nodes, $d\mathbf{q}_e/d\theta$ and $d\mathbf{q}_i/d\theta$, the unconditioned sensitivities of the generalized section deformations and section stress resultants are updated. The sensitivities of the section deformations are obtained using the compatibility relations, while the sensitivities of the section stress resultants are evaluated using the unconditional derivatives (with respect to the sensitivity parameter θ) of the material constitutive relations, i.e.,

$$\frac{dN_\alpha}{d\theta} = \int_{A_\alpha}\frac{d\sigma[y,\varepsilon_\alpha(z,\theta),\chi(z,\theta),\theta]}{d\theta}dA, \quad \alpha = 1,2 \tag{29}$$

$$\frac{dM_{12}}{d\theta} = \sum_{\alpha=1}^{2}\left\{\int_{A_\alpha}(y-y_\alpha)\frac{d\sigma[y,\varepsilon_\alpha(z,\theta),\chi(z,\theta),\theta]}{d\theta}dA\right\} \tag{30}$$

Response Sensitivity Analysis at the Material Level

For every (discretized) material constitutive model, the conditional and unconditional derivatives of the material state/history variables must be evaluated analytically with respect to the relevant material (sensitivity) parameters. This can be a challenging task when complex cyclic constitutive models are adopted, as is the case in this paper. The constitutive law used for the steel of the beam and for the reinforcements in the concrete slab is a uniaxial cyclic plasticity model with the von Mises yield criterion in conjunction with linear kinematic and isotropic hardening laws. This is the well-known bilinear inelastic material constitutive model. Detailed formulation and differentiation of this model can be found in Conte et al. (2003). The parameters of this material model consist of (1) Young's modulus of elasticity E_0, (2) the initial yield stress f_y, (3) the linear kinematic hardening modulus H_k, and (4) the linear isotropic hardening modulus H_i.

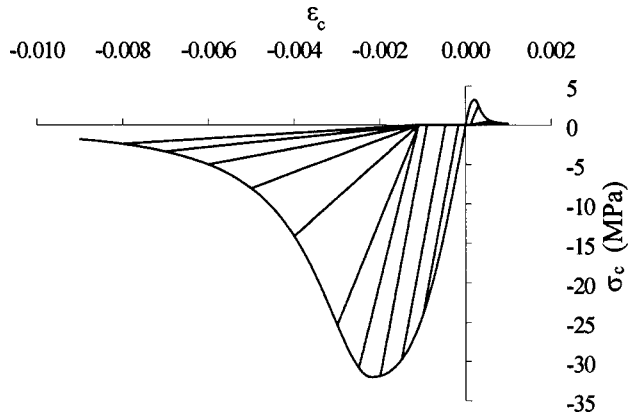

Fig. 2. Hysteretic concrete material model

The selected constitutive law for the concrete material is a uniaxial cyclic law with a monotonic envelope given by the Popovics–Saenz law (Balan et al. 1997, 2001; Kwon and Spacone 2002). A typical cyclic response of the concrete material model adopted herein is given in Fig. 2. Detailed formulation and differentiation of this model can be found in Zona et al. (2004). The parameters of this material model consist of (1) the initial modulus of elasticity E_c, (2) the compressive strength f_c and (3) the corresponding strain ε_0, (4) the stress f_f, and (5) the corresponding strain ε_f of the control point (inflection point) of the softening branch.

The constitutive law used for the shear connectors is a slip-force cyclic law with the monotonic envelope given by the Ollgaard et al. (1971) law. The cyclic response of the shear connectors is a modified version of the model proposed by Eligehausen et al. (1983) and is similar to the model used by Salari and Spa-

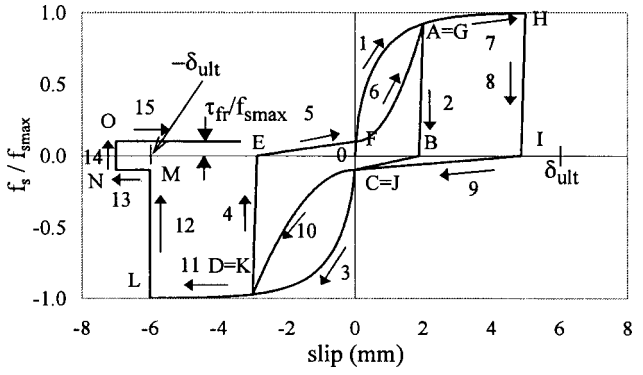

Fig. 3. Hysteretic model of shear connection

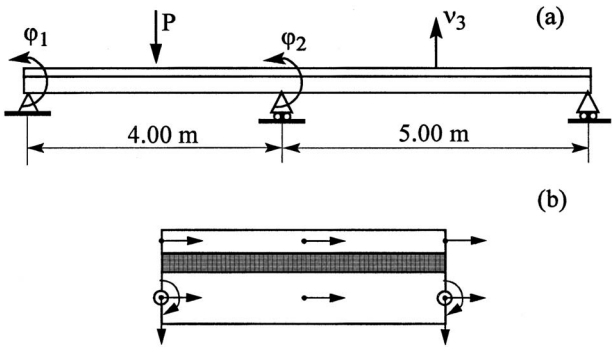

Fig. 4. (a) Configuration of the Ansourian CTB1 continuous beam and (b) degrees of freedom of the 10-DOF composite beam element used

cone (2001). A typical cyclic response of the constitutive model for the shear connectors used in this study is shown in Fig. 3. Detailed formulation and differentiation of this model can be found in Zona et al. (2004). The parameters of the connection "material" model consist of (1) the connection strength f_{smax}, (2) the ultimate slip δ_{ult}, and (3) the friction parameter τ_{fr}, see Fig. 3.

Computer Implementation

The above formulation for finite element response sensitivity analysis using composite beam elements with deformable shear connection was implemented in *FEDEASLab* (Filippou and Constantinides, 2004), a general-purpose nonlinear finite element structural analysis program. *FEDEASLab* is a *Matlab* (Math Works 1997) toolbox suitable for linear and nonlinear, static and dynamic structural analysis, which provides a general framework for physical parameterization of finite element models and response sensitivity computation (Franchin 2004).

Validation Examples

Nonlinear Monotonic Quasi-static Test

The first benchmark problem considered is a nonsymmetric two-span continuous beam (Fig. 4), tested by Ansourian (1981) under monotonic quasi-static loading. The beam, denoted CTB1 in Ansourian (1981), has two spans 4.00 and 5.00 m long and is subjected to a vertical concentrated load P applied at the midpoint of the shorter span. The joist section is a European IPE200; the reinforced concrete slab section is 100×800 mm^2. Due to the relatively narrow width of the concrete slab, shear lag effects are neglected in its modeling. The reader is referred to Ansourian (1981) for all details regarding the geometry and material properties. This problem presents all the main difficulties typically encountered in the analysis of steel-concrete composite structures, such as concrete softening in compression, concrete cracking in tension, and high gradients of slip and shear force along the connection (Dall'Asta and Zona 2002, 2004c). The structure is discretized uniformly into 18 10-DOF elements, see Fig. 4, with five Gauss–Lobatto points each (Dall'Asta and Zona 2003, 2004c). A quasi-static, monotonic, materially nonlinear-only analysis of the beam structure is performed using the incremental-iterative procedure defined above in displacement-control mode with the vertical displacement at the point of application of the load taken as the controlled DOF, thus mimicking the physical experiment. The computed load-deflection curves for the two spans are shown in Fig. 5, where they are compared with the experimental results. It is observed that the analytical predictions are in very good agreement with the experimental results. It is worth mentioning that in spite of the fact that the loading is monotonic, small unloading and reloading events are experienced at a few Gauss–Lobatto points due to internal stress redistribution. However, these events do not significantly affect the overall response, i.e., practically the

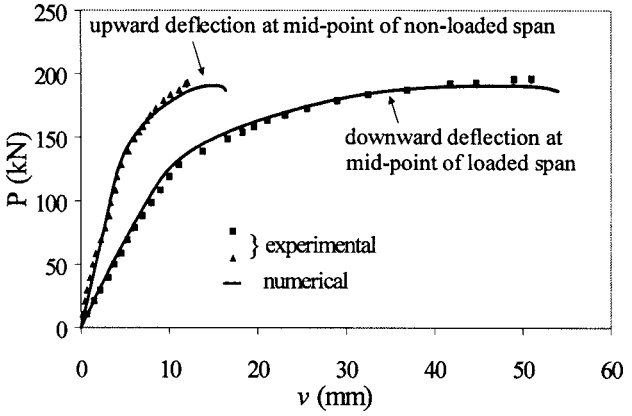

Fig. 5. Beam CTB1: load-deflection curves

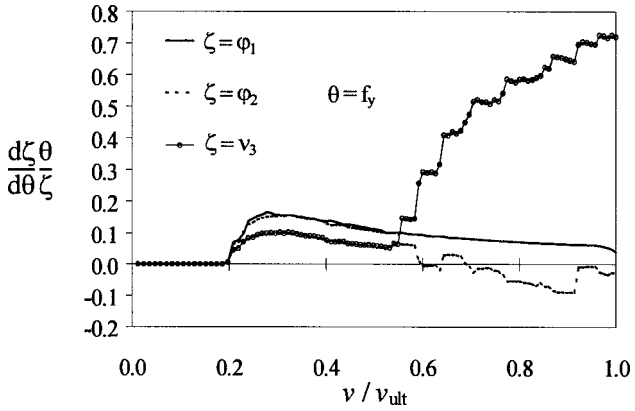

Fig. 6. Beam CTB1: global response sensitivities to f_y

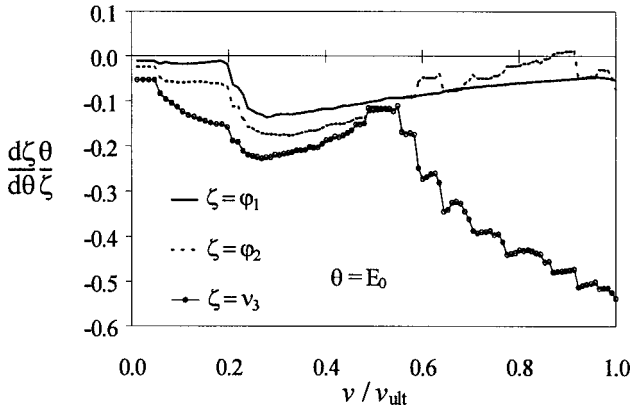

Fig. 7. Beam CTB1: global response sensitivities to E_0

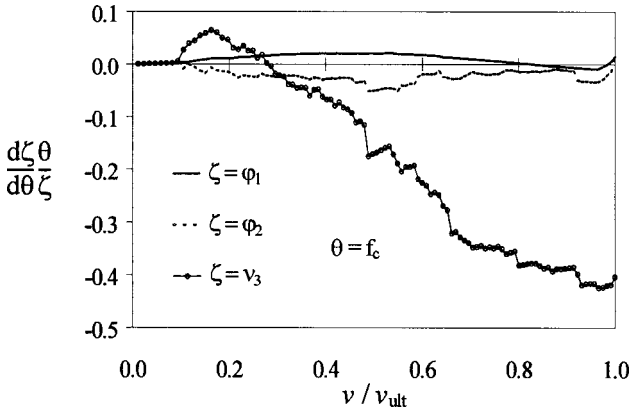

Fig. 8. Beam CTB1: global response sensitivities to f_c

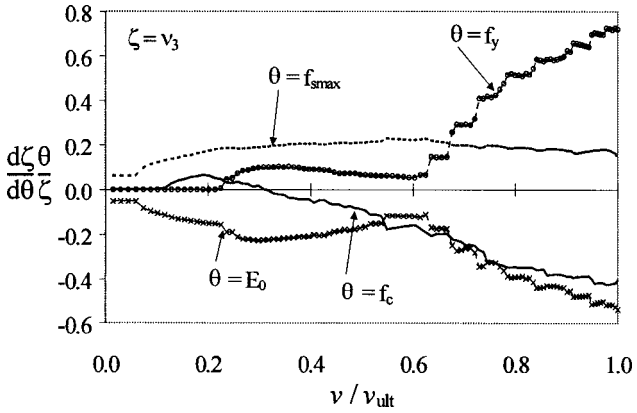

Fig. 10. Beam CTB1: Sensitivity of global response υ_3 to f_y, E_0, f_c, and f_{smax}

same results are obtained with nonlinear elastic constitutive laws with the same monotonic envelope neglecting the cyclic behavior (Dall'Asta and Zona 2003, 2004c).

Sensitivities of various global and local response quantities to all material parameters were computed using DDM and FFD. Due to space limitation, only the sensitivities to the most important material parameters (i.e., the parameters to which the response in question is most sensitive) are shown below. The reader is referred to Zona et al. (2004) for an exhaustive presentation of the response sensitivity analysis. The sensitivity results are presented in normalized form, i.e., multiplied by the value of the sensitivity parameter and divided by the value of the response quantity itself. Thus the normalized sensitivities represent the percent variation of the subject response quantity for a unitary percent variation of the sensitivity parameter. In this way, the normalized response sensitivities reveal directly the relative importance of all the material parameters considered in regards to a given response quantity at various loading stages of the structure.

Sensitivities of three global response quantities (i.e., rotation φ_1 at the left support, rotation φ_2 at the intermediate support, and deflection ν_3 at midpoint of the nonloaded span, see Fig. 4) to the four most important parameters (i.e., modulus of elasticity E_0 and yield stress f_y of the steel beam material, compressive strength f_c of the concrete, and strength f_{smax} of the shear connection) are shown in Figs. 6–9. The sensitivities are plotted as functions of the ratio of the deflection ν at midpoint of the loaded span to its value at collapse ν_{ult} predicted analytically (collapse being defined as the point at which the ultimate strain or the ultimate slip is reached for the first time along any of the material fibers or along the shear connection, respectively). It can be observed that the response sensitivities to f_y are null before yielding occurs for the first time (Fig. 6) as expected since prior to first yield, f_y does not affect the response. Some of the response sensitivities are characterized by strong discontinuities, due to material state transitions from the elastic to the plastic regime at Gauss–Lobatto point (Conte 2001; Conte et al. 2003, 2004). These discontinuities appear to be strongly dependent on the load level. The jagged response sensitivities obtained are the manifestation of a complex structural behavior in which important redistributions of deformation and stress occur between the steel beam and the reinforced concrete slab through the shear connection, which behaves nonlinearly from very small slip values. Among the three degrees of freedom considered, the vertical deflection ν_3 at midpoint of the nonloaded span is the most sensitive response quantity for every parameter considered. This can be explained in part by the fact that ν_3 is more distant from the controlled degree of freedom than the other two degrees of freedom considered. The sensitivities of the displacement along the controlled degree of freedom (i.e., vertical displacement at the point of application of the load) are always zero.

The normalized sensitivities of ν_3 to the four material parameters considered are compared in Fig. 10. In this way, it is possible to clearly highlight and quantify the relative importance of the various material parameters at different load levels. For ex-

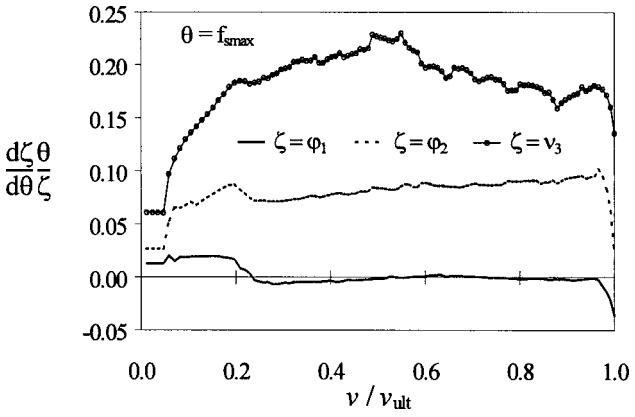

Fig. 9. Beam CTB1: global response sensitivities to f_{smax}

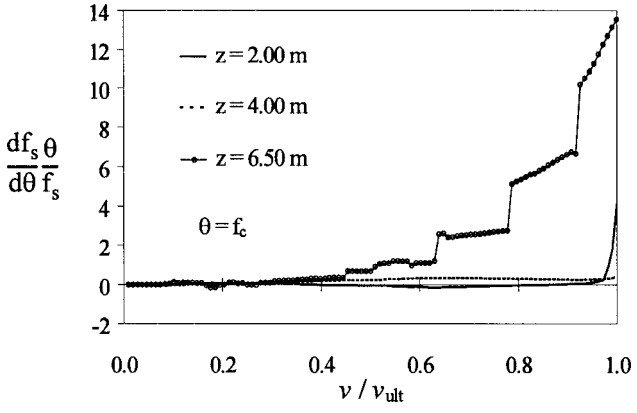

Fig. 11. Beam CTB1: sensitivity of shear force f_s (at different locations) to f_c

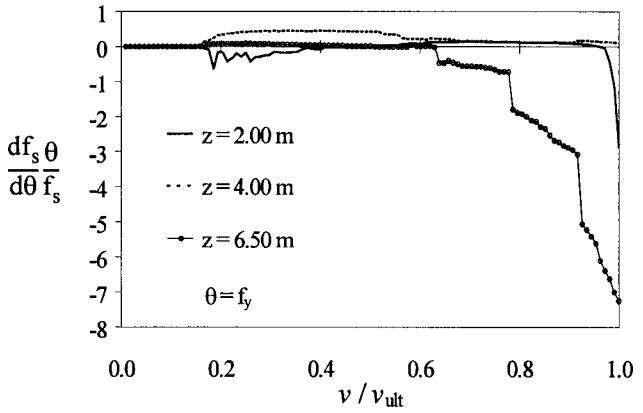

Fig. 12. Beam CTB1: sensitivity of shear force f_s (at different locations) to f_y

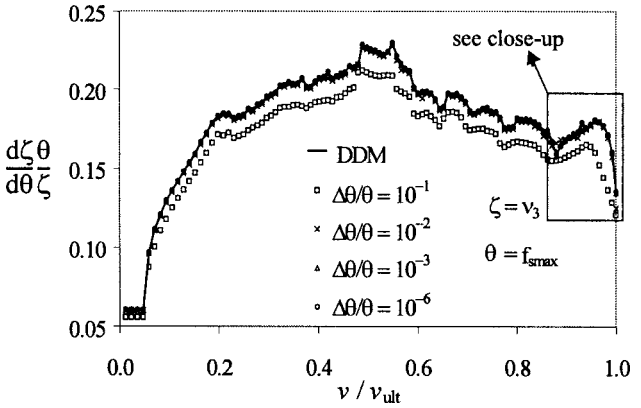

Fig. 15. Beam CTB1: sensitivity of midspan deflection v_3 to f_{smax} using direct differentiation method and forward finite difference

ample, it can be observed that the sensitivities to E_0 and f_{smax} are the most important at the early stage of the loading history, while as yielding spreads along the steel beam, material parameter f_y becomes increasingly important relative to the other parameters. Similar considerations apply to material parameter f_c, to which the sensitivity of v_3 increases significantly with increasing load level, even though the strength parameter f_c remains less important than the strength parameter f_y at high load levels.

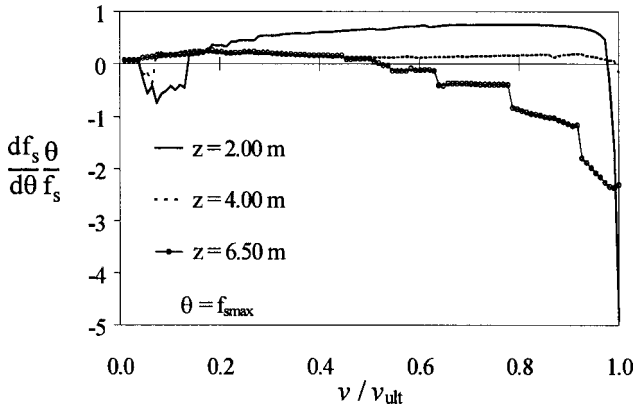

Fig. 13. Beam CTB1: sensitivity of shear force f_s (at different locations) to f_{smax}

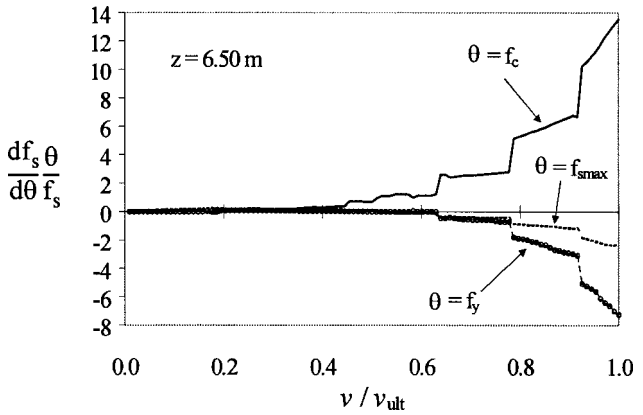

Fig. 14. Beam CTB1: sensitivity of shear force f_s (at z=6.50 m) to f_c, f_y, and f_{smax}

Sensitivities of a local response quantity (i.e., shear force per unit length f_s) at three locations (i.e., midpoint of the loaded span at z=2.00 m, intermediate support at z=4.00 m, and midpoint of the nonloaded span at z=6.50 m) to the three most important material parameters (i.e., yield stress f_y of the steel beam, compressive strength f_c of the concrete, shear connection strength f_{smax}) are plotted in Figs. 11–13. The sensitivities of f_s

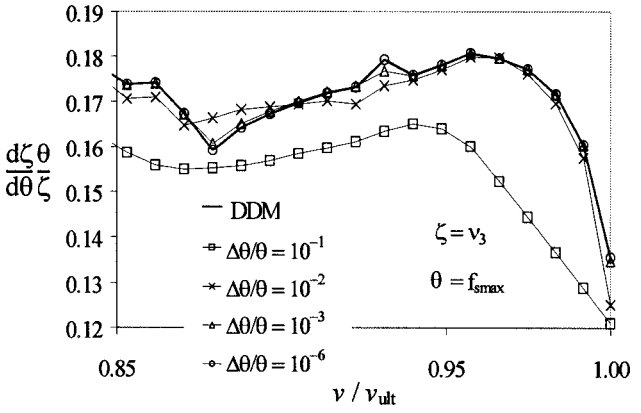

Fig. 16. Beam CTB1: sensitivity of midspan deflection v_3 to f_{smax} using direct differentiation method and forward finite difference (closeup)

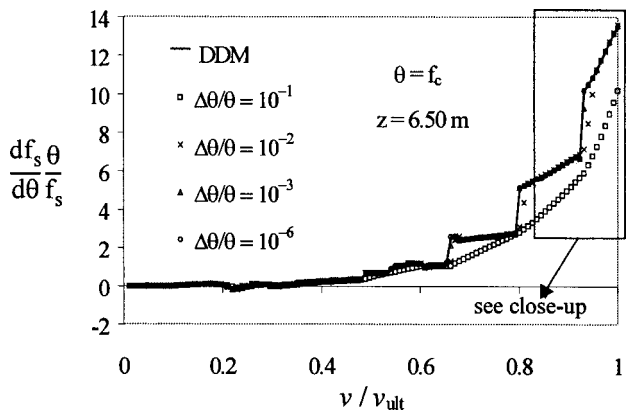

Fig. 17. Beam CTB1: sensitivity of shear force f_s to f_c using direct differentiation method and forward finite difference

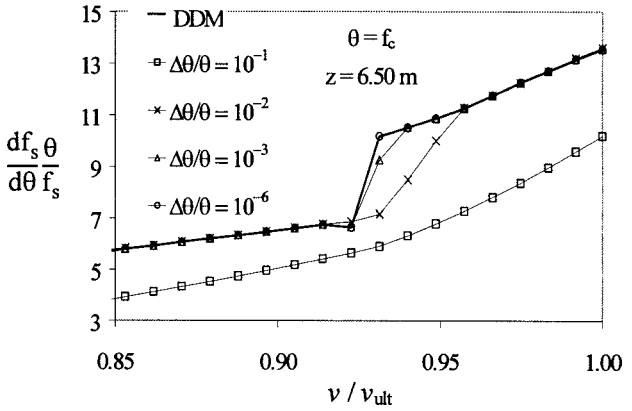

Fig. 18. Beam CTB1: sensitivity of shear force f_s to f_c using direct differentiation method and forward finite difference (closeup)

(at $z=6.50$ m) to the three material parameters f_y, f_c, and f_{smax} are plotted together in Fig. 14, clearly highlighting the relative importance of these three parameters. It is noteworthy that the discontinuities due to material state transitions (elastic-to-plastic) are more pronounced than at the global response level. It is also observed that at high load level ($v/v_{ult}>0.7$), the sensitivities of

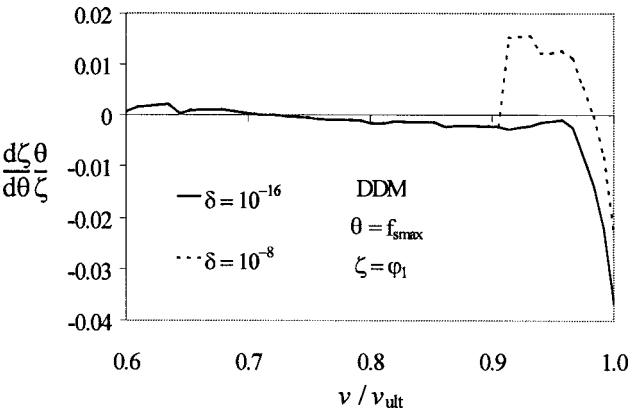

Fig. 19. Beam CTB1: effect of convergence tolerance for response calculation on direct differentiation method results

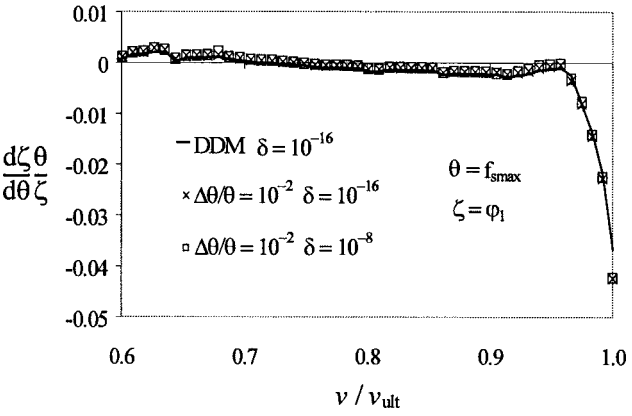

Fig. 20. Beam CTB1: effect of convergence tolerance for response calculation on agreement between response sensitivity results obtained using direct differentiation method and forward finite difference (case in which forward finite difference results converge to direct differentiation method results)

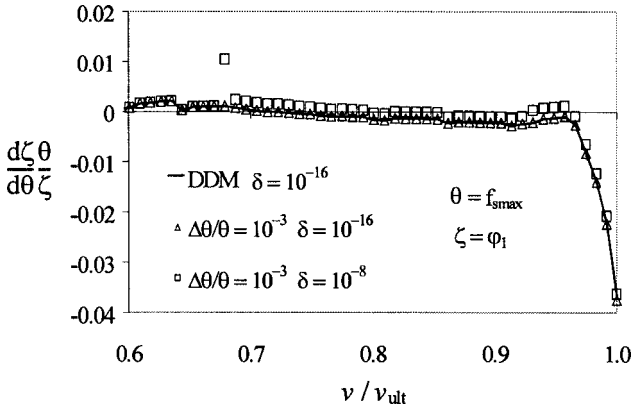

Fig. 21. Beam CTB1: effect of convergence tolerance for response calculation on agreement between response sensitivity results obtained using direct differentiation method and forward finite difference (case in which forward finite difference results do not converge to direct differentiation method results)

the local response f_s increase more strongly with the load level than the global response sensitivities previously considered (see Figs. 6–10).

All the sensitivity results shown were computed using the DDM and validated by the FFD method using increasingly small perturbations of the sensitivity parameter. Due to space limitations, the comparison between DDM and FFD results is shown

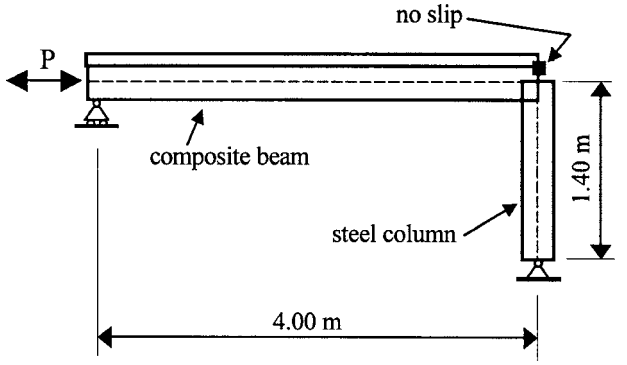

Fig. 22. Frame intermediate partial connection: configuration of test specimen

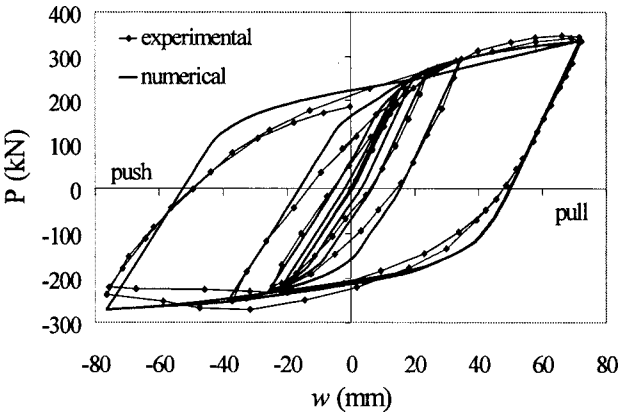

Fig. 23. Frame intermediate partial connection: load-deflection curves

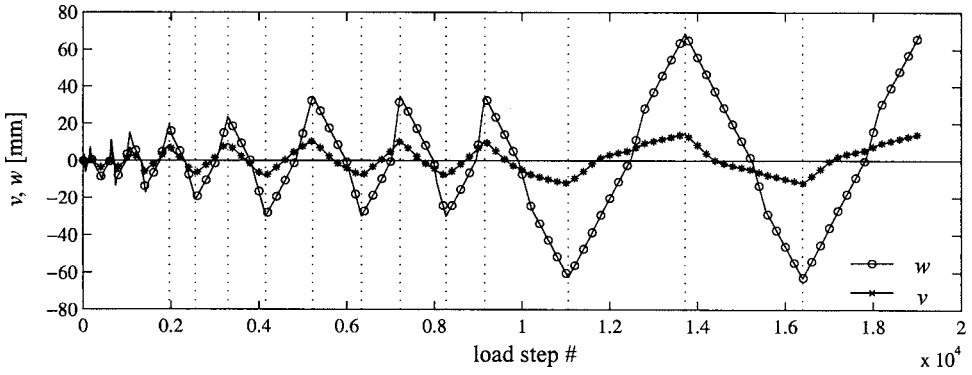

Fig. 24. Frame intermediate partial connection: vertical displacement v at midspan and horizontal displacement w at the right end of the beam as functions of the load step number

herein only for two cases. The first case considered is the sensitivity of the deflection v_3 of the nonloaded span to the shear connection strength $f_{s\max}$ (Fig. 15 and closeup in Fig. 16); four levels of perturbation of parameter $f_{s\max}$ were considered, namely $\Delta\theta/\theta=10^{-1}$, 10^{-2}, 10^{-3}, and 10^{-6}. The second case considered is the sensitivity of the interface shear force f_s at midspan of the nonloaded span ($z=6.50$ m) to the concrete compressive strength f_c (Fig. 17 with closeup in Fig. 18). The same four levels of perturbation were considered for parameter f_c ($\Delta\theta/\theta=10^{-1}$, 10^{-2}, 10^{-3}, and 10^{-6}). In both cases, it is shown that the FFD results converge asymptotically to the DDM results as $\Delta\theta/\theta$ becomes increasingly small, and that the FFD results for $\Delta\theta/\theta=10^{-3}$ are close to the DDM results.

Figs. 19–21 show the effects of the prescribed tolerance δ (used in the energy-based convergence criterion for response calculation) upon convergence of the FFD sensitivity results to their DDM counterparts. In these figures, the response quantity of interest is the rotation φ_1 of the left end node of the two-span continuous beam and the sensitivity parameter θ is the shear connection strength $f_{s\max}$. The sensitivity results are plotted for $\nu/\nu_{\text{ult}}>0.6$. Global and local response sensitivities might present irregularities such as the one plotted in Fig. 19 where the sensitivity is plotted for an insufficiently small tolerance ($\delta=10^{-8}$) and for the small tolerance $\delta=10^{-16}$, which was found to be the largest tolerance leading to the correct DDM results. Fig. 20 shows the sensitivity results obtained through FFD analysis with a perturbation $\Delta f_{s\max}/f_{s\max}=10^{-2}$ with $\delta=10^{-8}$ and 10^{-16}, respectively, compared with the DDM results (obtained using $\delta=10^{-16}$); in this case, no difference can be noticed between the FFD results obtained using two different values of the tolerance δ (i.e., $\delta=10^{-8}$ and 10^{-16}). Fig. 21 shows the same sensitivity results, but using a perturbation $\Delta f_{s\max}/f_{s\max}=10^{-3}$ for the FFD analysis. In this case, it is noticed that the FFD results are not in good agreement with the DDM results when an insufficiently small tolerance ($\delta=10^{-8}$) is adopted for the iterative response calculation. This example and other examples in Zona et al. (2004) show that the choice of a strict enough convergence tolerance for the iterative response calculation is important for response sensitivity analysis, since Eq. (2) is the starting point of the DDM. Use of an inadequate convergence tolerance for response calculation may lead to loss of agreement between response sensitivity results obtained using the DDM and FFD analysis (e.g., an insufficiently small convergence tolerance δ can lead to erroneous DDM results and very inaccurate FFD results if the perturbation of the sensitivity parameter is "too small" in relation to δ).

Nonlinear Cyclic Quasi-static Test

The second benchmark problem considered is a frame subassemblage tested by Bursi and Gramola (2000) subjected to quasi-static cyclic loading (Fig. 22). The frame subassemblage, denoted as IPC (intermediate partial connection) in Bursi and Gramola (2000), has a steel-concrete composite beam 4.00 m long made of a European IPE300 steel section and a reinforced concrete slab 1,200 mm wide. The shear-lag effects are considered in a simplified way by reducing the slab width to 820 mm over the entire length of the beam (Bursi and Gramola 2000). The steel column is a European HE360B section. The reader is referred to Bursi and Gramola (2000) for all details regarding the geometry, material properties, and the loading history. This subassemblage is repre-

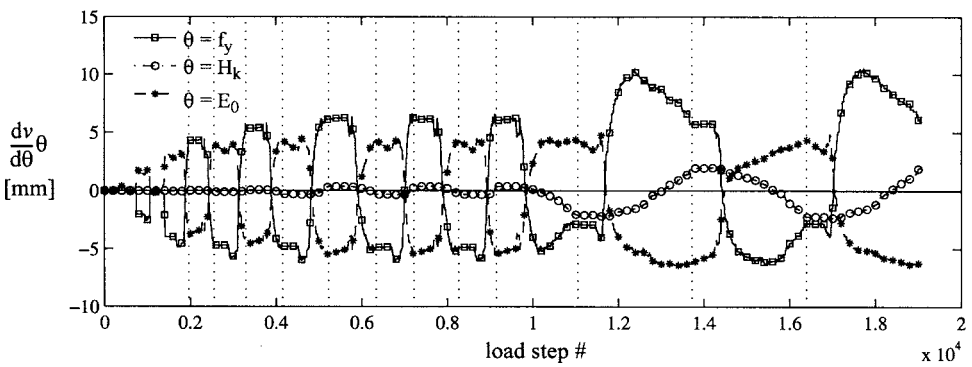

Fig. 25. Frame intermediate partial connection: sensitivities of the beam midspan vertical deflection v to steel beam material parameters

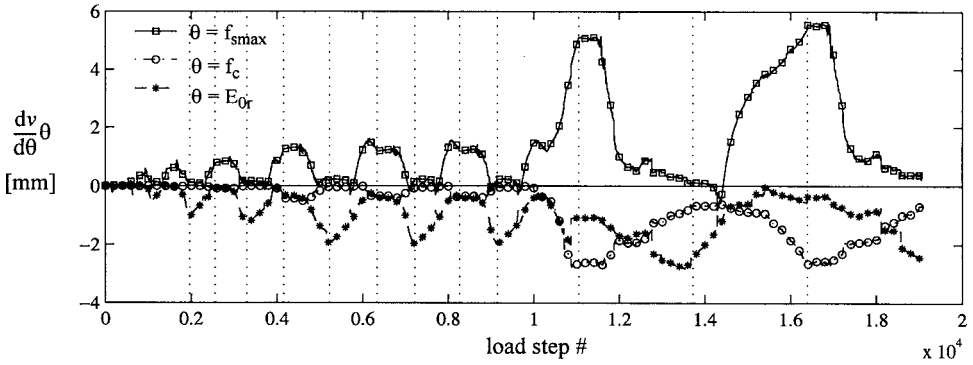

Fig. 26. Frame intermediate partial connection: sensitivities of the beam midspan deflection v to parameters related to concrete slab and shear connection

sentative of the behavior of steel-concrete composite frames adopted for seismic-resistant buildings. In addition to the difficulties encountered in the previous example, this case includes problems related to the more complex loading history which is cyclic.

The frame subassemblage is uniformly discretized into five 10-DOF composite frame elements for the beam and one frame element for the column. A materially nonlinear-only cyclic, quasi-static analysis of the frame subassemblage is performed using the incremental-iterative procedure defined above in displacement control mode with the horizontal displacement of the steel beam centroid at the left end of the beam selected as the controlled DOF (as in the experimental tests). The computed load-deflection curve is displayed in Fig. 23, where it is compared with the experimental results. It is observed that analytical and experimental results are in good agreement, despite the fact that the finite element model does not include the effects of local buckling (nonlinear geometry) in the steel beam during the push phase of the cyclic loading in the last set of cycles. The extra "fatness" of the computed hysteresis loops is due to the bilinear shape and lack of smoothness of the one-dimensional J_2 plasticity model used for the steel beam and the steel reinforcements in the concrete slab.

Sensitivities of various global and local response quantities to all material parameters were computed using DDM and FFD. Here, for the sake of brevity, only selected sensitivity results are presented. The response sensitivities are only multiplied by the value of the sensitivity parameter (and not divided by the value of

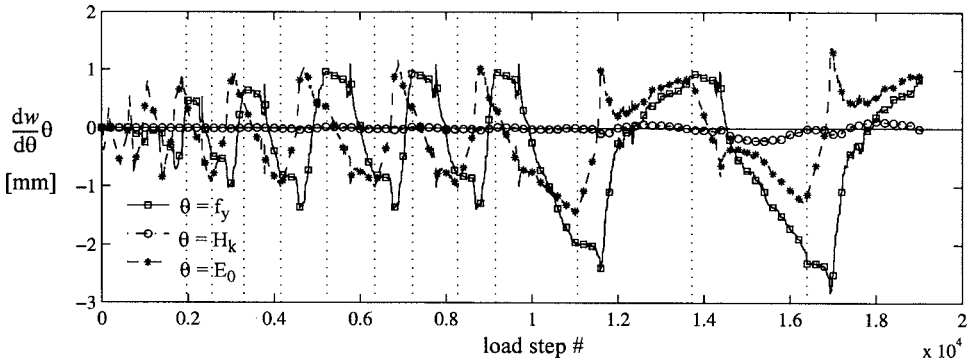

Fig. 27. Frame intermediate partial connection: sensitivities of the beam horizontal displacement w to steel beam material parameters

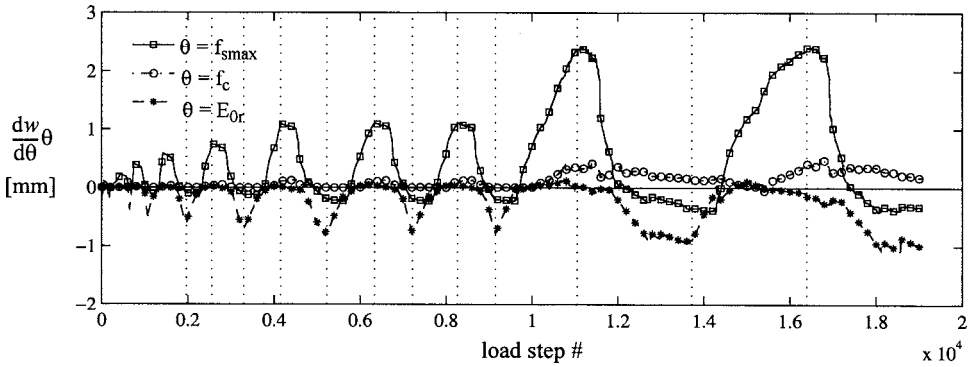

Fig. 28. Frame intermediate partial connection: sensitivities of the beam horizontal displacement w to parameters related to concrete slab and shear connection

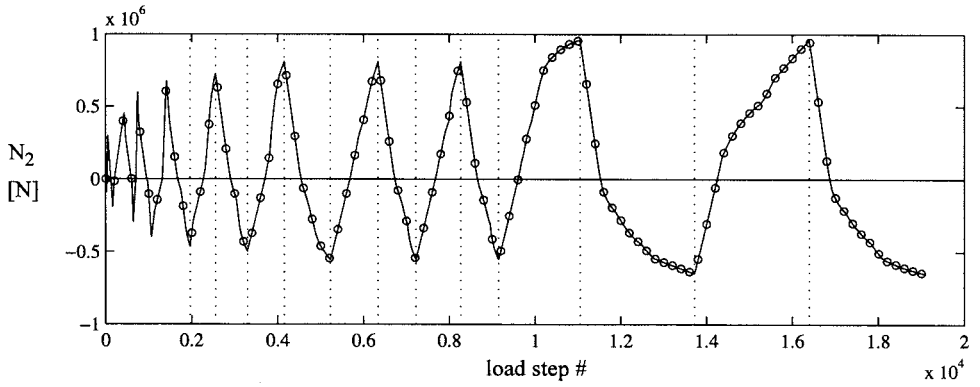

Fig. 29. Frame intermediate partial connection: axial force N_2 in the steel beam at midspan as a function of the load step number

the response which can be very small due to its cyclic nature). The normalized sensitivities can thus be interpreted as one hundred times the change in the subject response quantity for a unitary percent variation of the sensitivity parameter.

The global response quantities considered in this example are the horizontal displacement w of the steel beam centroid at the right-end of the beam and the vertical deflection v of the beam at midspan; their analytical predictions are plotted in Fig. 24 as functions of the load step number. The sensitivities of v are shown in Fig. 25 for the steel beam material parameters (i.e., θ=yield stress f_y, modulus of elasticity E_0, and kinematic hardening modulus H_k) and in Fig. 26 for material parameters related to the concrete slab and the shear connection (θ=shear connection strength f_{smax}, concrete compressive strength f_c, and modulus of elasticity E_{0r} of the steel reinforcements). Similarly, the sensitivities of w are shown in Fig. 27 ($\theta=f_y,E_0,H_k$) and in Fig. 28 ($\theta=f_{smax},f_c,E_{0r}$). It was found (Zona et al. 2004) that the two DOFs v and w are most sensitive to the steel beam parameters (f_y,E_0,H_k) and the shear connection strength f_{smax}.

The local response quantity considered here is the axial force N_2 in the steel beam at midspan which is plotted in Fig. 29 as a function of the load step number. The sensitivities of this local response quantity to $\theta=f_y,f_{smax},f_c$ are shown in Fig. 30. These three material parameters control the inelastic behavior of each component (steel beam, shear connection, and concrete slab) of the composite beam and thus influence the diffusion of the ap-

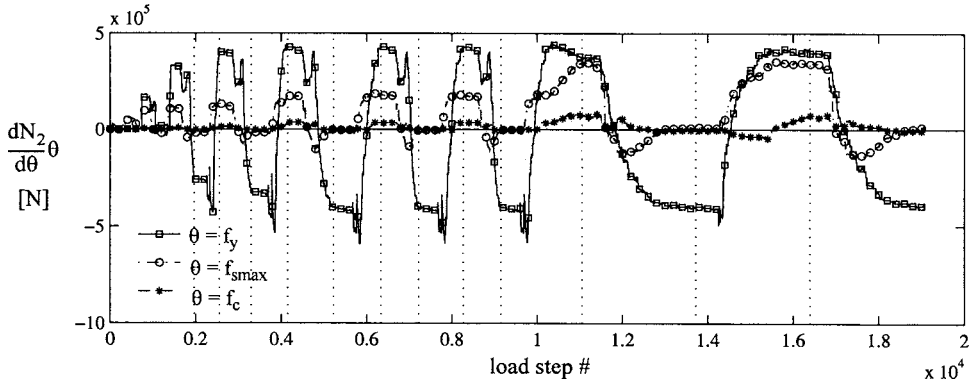

Fig. 30. Frame intermediate partial connection: sensitivities of axial force N_2 in the steel beam at midspan to f_y, f_{smax}, f_c

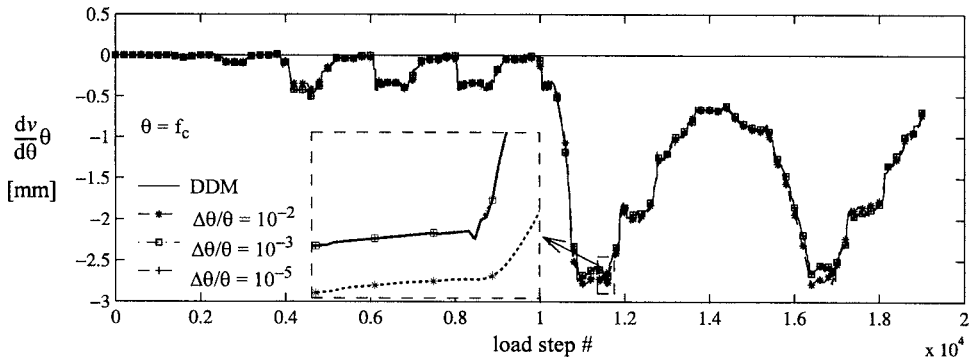

Fig. 31. Frame intermediate partial connection: sensitivities of vertical deflection v to f_c using direct differentiation method and forward finite difference

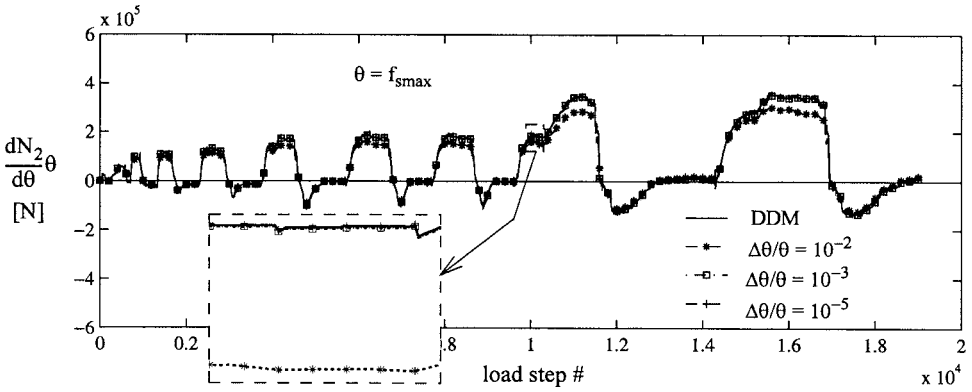

Fig. 32. Frame intermediate partial connection: sensitivities of the axial force N_2 to f_{smax} using direct differentiation method and forward finite difference

plied axial force from the steel beam to the concrete slab. It was found that for N_2, f_y is once again the most important response parameter (Zona et al. 2004). The sensitivities of N_2 as well as other internal forces (shear, bending moment) to most of the material parameters were found to be very erratic (high frequency spikes and discontinuities).

The vertical dotted lines in Figs. 24–30 mark the end of the last loading step or beginning of the first unloading step. Careful examination of the results revealed that no discontinuities occurred exactly at unloading events. This is consistent with prior results on simpler benchmark problems (Conte et al. 2003). It thus appears that discontinuities in finite element response sensitivities are due to material state transitions from elastic to plastic and not vice versa.

All the sensitivity results presented were computed using the DDM and validated by FFD using increasingly small perturbations of the sensitivity parameters. Due to space limitation, the comparison between DDM and FFD results is shown here only for two cases. The first case consists of the sensitivity of the vertical deflection v at midspan to the concrete strength f_c (Fig. 31). For the FFD analysis, three levels of perturbation of parameter f_c were considered, namely $\Delta\theta/\theta=10^{-2}$, 10^{-3}, and 10^{-5}. The second case consists of the sensitivity of the axial force N_2 in the steel beam at midspan to the shear connection strength f_{smax} (Fig. 32). The same three levels of perturbation (i.e., $\Delta\theta/\theta=10^{-2}$, 10^{-3}, and 10^{-5}) were considered for parameter f_{smax}. From these two figures and their closeups, the FFD results are shown to converge asymptotically to their DDM counterparts as the perturbation of the sensitivity parameter becomes increasingly small. In these two cases, the FFD results are converged to the DDM results for $\Delta\theta/\theta=10^{-5}$.

Conclusions

This paper focuses on materially nonlinear-only analytical response sensitivity analysis, using displacement-based finite elements in conjunction with the direct differentiation method (DDM), of composite beams with deformable shear connection under quasi-static monotonic and cyclic loading conditions. Realistic uniaxial constitutive models are used for the steel and concrete materials as well as for the shear connection. The concrete and shear connection material models as well as the static condensation procedure at the element level are extended for response sensitivity computations using the DDM. Two benchmark problems that have been the object of experimental testing are used to illustrate the proposed methodology for response sensitivity analysis. The first benchmark problem consists of a two-span asymmetric continuous beam subjected to monotonic loading with a concentrated force. The second benchmark problem consists of a frame subassemblage subjected to quasi-static cyclic loading. The finite element response prediction is validated using experimental results available in the literature for the two benchmark problems. The response sensitivity analysis results obtained according to the direct differentiation method (DDM) are validated by means of forward finite difference (FFD) analysis. Selected results of response sensitivity analysis are presented in an effort to quantify the effect and relative importance of various material constitutive model parameters in regards to the nonlinear quasi-static monotonic and cyclic response of a tested steel-concrete composite beam. Using the benchmark problem considered, it is also shown that use of an inadequate convergence tolerance in the nonlinear finite element response calculation may introduce numerical errors in response sensitivity analysis results obtained using both the DDM and FFD analysis.

The algorithms developed in this study for nonlinear finite element response sensitivity analysis of steel-concrete composite structures have direct applications in structural optimization, structural reliability analysis, and nonlinear finite element model updating for this type of structure.

Acknowledgments

Partial supports of this research by the National Science Foundation under Grant No. CMS-0010112 and by the Pacific Earthquake Engineering Research (PEER) Center through the Earthquake Engineering Research Centers Program of the National Science Foundation under Award No. EEC-9701568 are gratefully acknowledged. This work was also partially supported by the National Center for Supercomputing Applications (NCSA) under Grant No. MSS040022N and utilized the IBM P690. The writers wish to thank Professor Filip C. Filippou at the University of California, Berkeley, and Dr. Paolo Franchin at the University of Rome "La Sapienza," Italy, for providing them with the *Matlab*-based nonlinear structural analysis framework, *FEDEASLab*, used in this study together with the added framework for finite element response sensitivity analysis. The writers also want to acknowledge Professor Enrico Spacone at the University "G. D'Annunzio" of Chieti, Italy, and Dr. Reza Salari at RockSol

Consulting Group, Inc., Boulder, Colo., for very useful discussions and suggestions regarding the finite element modeling part of this work. In addition, the first writer wishes to thank Professor Luigino Dezi at the Università Politecnica delle Marche, Italy, and Professor Andrea Dall' Asta at the University of Camerino, Italy, for their personal and financial support.

References

Ansourian, P. (1981). "Experiments on continuous composite beams." *Proc. Inst. Civil Eng. Part 2*, 71, 25–51.

Balan, T. A., Filippou, F. C., and Popov, E. P. (1997). "Constitutive model for 3D cyclic analysis of concrete structures." *J. Eng. Mech.*, 123(2), 143–153.

Balan, T. A., Spacone, E., and Kwon, M. (2001). "A 3D hypoplastic model for cyclic analysis of concrete structures." *Eng. Struct.*, 23, 333–342.

Bathe, K. J. (1995). *Finite element procedures*, Prentice-Hall, Englewood Cliffs, N.J.

Bursi, O. S., and Gramola, G. (2000). "Behaviour of composite substructures with full and partial shear connection under quasi-static cyclic and pseudo-dynamic displacements." *Mater. Struct.*, 33, 154–163.

Conte, J. P. (2001). "Finite element response sensitivity analysis in earthquake engineering." *Earthquake engineering frontiers in the new millennium*, Spencer & Hu, Swets & Zeitlinger, Lisse, The Netherlands, 395–401.

Conte, J. P., Barbato, M., and Spacone, E. (2004). "Finite element response sensitivity analysis using force-based frame models." *Int. J. Numer. Methods Eng.*, 59(13), 1781–1820.

Conte, J. P., Vijalapura, P. K., and Meghella, M. (2003). "Consistent finite element response sensitivity analysis." *J. Eng. Mech.*, 129(12), 1380–1393.

Dall'Asta, A. (2001). "Composite beams with weak shear connection." *Int. J. Solids Struct.*, 38, 5605–5624.

Dall'Asta, A., and Zona, A. (2002). "Non-linear analysis of composite beams by a displacement approach." *Comput. Struct.*, 80, 27–30; 2217–2228.

Dall'Asta, A., and Zona, A. (2003). "Evaluation of finite elements for the study of the ultimate behaviour of steel-concrete composite beams." *Proc., Int. Conf. of Advances in Structures: Steel, Concrete, Composites and Aluminium*, G. J. Hancock, M. A. Bradford, T. J. Wilkinson, B. Uy, and K. J. R. Rasmussen, eds., A. A. Balkema Publishers—Swets & Zeitlinger B.V., Lisse, The Netherlands, 703–709.

Dall'Asta, A., and Zona, A. (2004a). "Three-field mixed formulation for the non-linear analysis of composite beams with deformable shear connection." *Finite Elem. Anal. Design*, 40(4), 425–448.

Dall'Asta, A., and Zona, A. (2004b). "Slip locking in finite elements for composite beams with deformable shear connection." *Finite Elem. Anal. Design*, 40(13–14), 1907–1930.

Dall'Asta, A., and Zona, A. (2004c). "Comparison and validation of displacement and mixed elements for the non-linear analysis of continuous composite beams." *Comput. Struct.*, 82(23-26), 2117–2130.

Dall'Asta, A., and Zona, A. (2005). "Finite element model for externally prestressed composite beams with deformable connection." *J. Struct. Eng.*, 131(5), 706–714.

Ditlevsen, O., and Madsen, H. O. (1996). *Structural reliability methods*, Wiley, New York.

Eligehausen, R., Popov, E. P., and Bertero, V. V. (1983). "Local bond stress-slip relationships of deformed bars under generalized excitations." *Rep. No. 83/23*, EERC Earthquake Engineering Research Center, Univ. of California, Berkeley, Calif., 162.

Filippou, F. C., and Constantinides, M. (2004). "FEDEASLab Getting Started Guide and Simulation Examples." Technical Report NEESgrid-2004-22. <www.neesgrid.org>

Franchin, P. (2004). "Reliability of uncertain inelastic structures under earthquake excitations." *J. Eng. Mech.*, 130(2), 1–12.

Kleiber, M., Antunez, H., Hien, T. D., and Kowalczyk, P. (1997). *Parameter sensitivity in nonlinear mechanics: Theory and finite element computations*, Wiley, New York.

Kwon, M., and Spacone, E. (2002). "Three-dimensional finite element analyses of reinforced concrete columns." *Comput. Struct.*, 80, 199–212.

MathWorks Inc. (1997). "*Matlab*—High performance numeric computation and visualization software." *User's guide*, Natick, Mass.

Newmark, N. M., Siess, C. P., and Viest, I. M. (1951). "Tests and analysis of composite beams with incomplete interaction." *Proc. Soc. Exp. Stress Anal.*, 9(1), 75–92.

Oehlers, D. J., and Bradford, M. A. (2000). *Elementary behaviour of composite steel and concrete structural members*, Butterworth-Heinemann, London.

Ollgaard, J. G., Slutter, R. G., and Fisher, J. W. (1971). "Shear strength of stud connectors in lightweight and normal weight concrete." *AISC Eng. J.*, 2Q, 55–64.

Salari, M. R., and Spacone, E. (2001). "Analysis of steel-concrete composite frames with bond-slip." *J. Struct. Eng.*, 127(11), 1243–1250.

Spacone, E., and El-Tawil, S. (2004). "Nonlinear analysis of steel-concrete composite structures: State-of-the-art." *J. Struct. Eng.*, 130(2), 159–168.

Zona, A., Barbato, M., and Conte, J. P. (2004). "Finite element response sensitivity analysis of steel-concrete composite structures." *Rep. No. SSRP-04/02*, Dept. of Structural Engineering, Univ. of California, San Diego.